AER210 Microfluidics Laboratory Report

Nicholas Nguyen
1010900474

November 12, 2025

Contents

1 Introduction **3**

2 Length Scale and Uncertainty **3**
2.1 Conversion of Image Distances to Physical Scale 3
2.2 Uncertainties in Length, Time, and Velocity 3
2.3 Uncertainty Propagation of Velocity 3
2.4 Non-Quantifiable Errors and Assumptions 3

3 Chip Design **4**
3.1 Imperfections and Their Flow Effects 4
3.2 Effects of Wall Imperfections 4

4 Straight Channels **4**
4.1 Flow Regime 4
4.2 Velocity Maximum and Gradient 5
4.3 Velocity Profile) 5
4.4 Expected Curve Type 5
4.5 Manipulating Mean Velocity 5
4.6 Velocity vs. Syringe Height 6
4.7 Hagen–Poiseuille: Symbolic Relationship 6
4.8 Bonus: Bernoulli Relation 6

5 Channels of Different Size **7**
5.1 Expected Velocity Ratio 7
5.2 Measured Ratio (Data Required) 7
5.3 Flow Features 7
5.4 Turbulence 7
5.5 Flow Transitions in Engineering 8

6 Channels with Bends **8**
6.1 Velocity Change 8
6.2 Flow Features 8
6.3 Turbulence 8
6.4 Concave vs. Convex Corners 8

7 Conclusion **9**

1 Introduction

This experiment introduces foundational principles of microfluidic flow, including laminar transport, channel geometry effects, and velocity visualization using fluorescent beads. Due to the microscale dimensions involved, inertial forces are typically small relative to viscous forces, resulting in low Reynolds numbers and highly ordered flows suitable for quantitative study.

2 Length Scale and Uncertainty

2.1 Conversion of Image Distances to Physical Scale

To convert pixel distances into physical length scales, an image with a known physical dimension (e.g. channel width) is used for calibration. A pixel-to-length ratio

$$\alpha = \frac{\text{known physical length}}{\text{measured pixel length}}$$

is obtained, and all measured lengths are multiplied by α to convert to physical units.

2.2 Uncertainties in Length, Time, and Velocity

Length uncertainties stem primarily from image resolution, focusing quality, and operator measurement error. Time uncertainty is dominated by the camera exposure-time specification and digitization precision. Velocity, computed by $v = d/t$, inherits uncertainty from both measured streak length and exposure duration.

2.3 Uncertainty Propagation of Velocity

Given

$$v = \frac{d}{t},$$

the relative uncertainty is

$$\left(\frac{\Delta v}{v}\right)^2 = \left(\frac{\Delta d}{d}\right)^2 + \left(\frac{\Delta t}{t}\right)^2.$$

Thus,

$$\Delta v = v\sqrt{\left(\frac{\Delta d}{d}\right)^2 + \left(\frac{\Delta t}{t}\right)^2}.$$

2.4 Non-Quantifiable Errors and Assumptions

Non-quantifiable effects include:

- Flow disturbances due to wall roughness
- Minor air bubbles altering local flow rates

- Entrance effects and non-ideal channel geometry
- Non-uniform bead distribution

These factors distort the ideal laminar velocity profile and complicate curve fitting.

3 Chip Design

3.1 Imperfections and Their Flow Effects

Imperfections (wall roughness, machining irregularities, debris) may cause local pressure losses. The resulting perturbations distort bulk velocity distribution and can introduce low-level turbulent intensity, increasing dissipation and mean pressure drop.

3.2 Effects of Wall Imperfections

Wall roughness leads to boundary-layer distortion. Locally, velocity gradients increase near protrusions, increasing drag and pressure drop downstream. Turbulence intensity can rise in regions with abrupt roughness change, referencing similar effects observed in the UTIAS wind tunnel.

4 Straight Channels

4.1 Flow Regime

At microfluidic length scales, Reynolds number is typically $\mathrm{Re} \ll 2000$, so laminar flow is expected. As seen in the captured images from the microfluidics lab, the smooth streaklines confirm laminar flow behavior in the straight tube section.

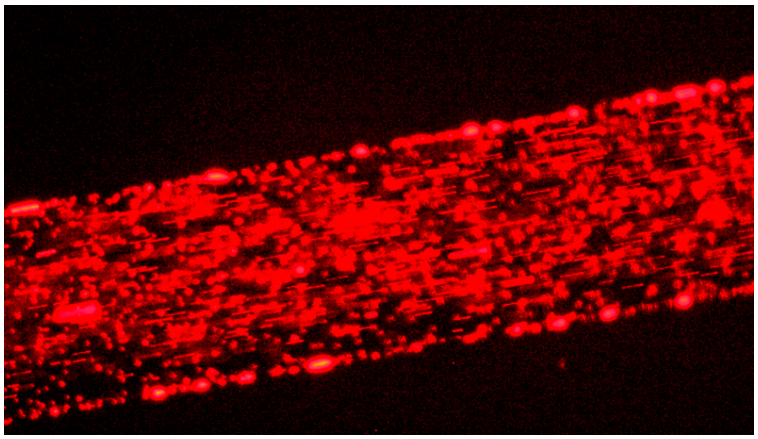

Figure 1: Straight channel streak visualization

4.2 Velocity Maximum and Gradient

For pressure-driven flow, maximum velocity occurs at channel centerline; the velocity gradient is largest near walls where no-slip applies. This matches theoretical parabolic Poiseuille flow. APG boundary-layer effects are not expected to play major roles in a straight microchannel.

4.3 Velocity Profile)

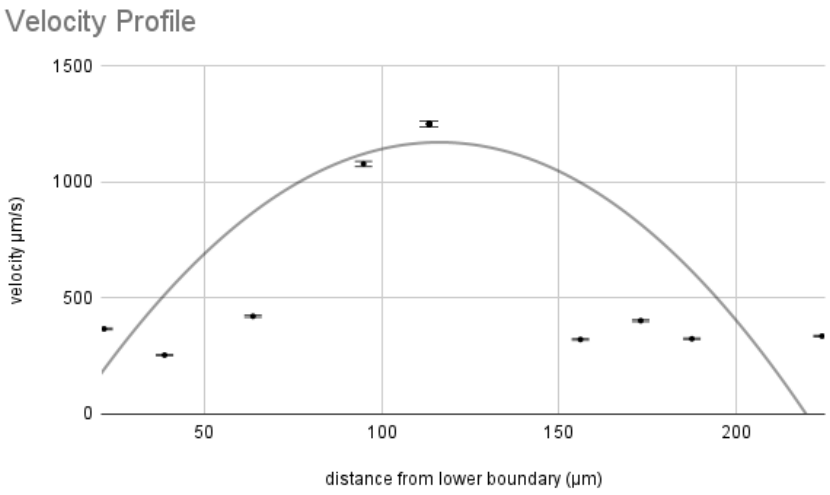

Figure 2: Velocity measurements of streaks at certain distances from the lower boundary of the straight channel. Parabola fitted to better depict the velocity profile.

4.4 Expected Curve Type

Theoretically, a parabolic velocity profile is expected for laminar channel flow.

4.5 Manipulating Mean Velocity

Mean velocity may be increased by:

- Raising the syringe height → increases hydrostatic pressure
- Lowering channel resistance → larger cross-section
- Increasing turbulence intensity (injecting disturbances)

Bernoulli's equation shows velocity increase is proportional to pressure difference.

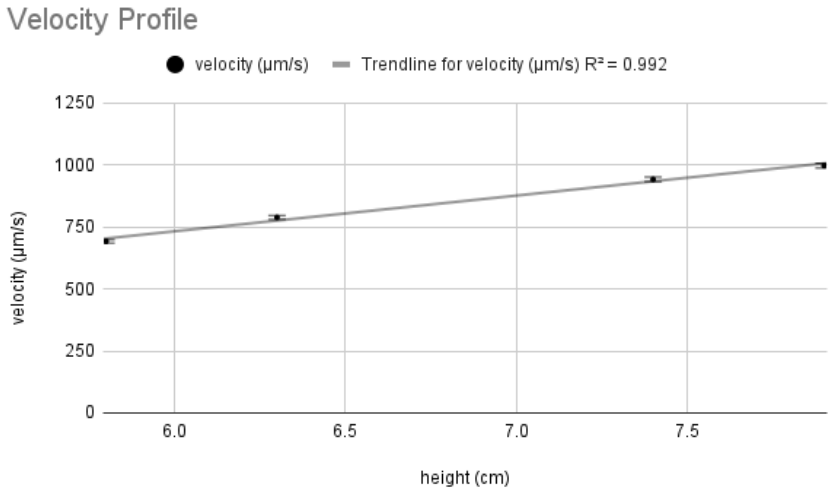

Figure 3: Velocity measurements taken at the same point in the center of the straight channel, with four varying heights of the syringe.

4.6 Velocity vs. Syringe Height

4.7 Hagen–Poiseuille: Symbolic Relationship

Hagen–Poiseuille gives

$$Q \propto \frac{\Delta p}{\mu L}, \quad Q = SU.$$

Since $\Delta p = \rho g z_1$,

$$U_3 \propto z_1.$$

Thus, fluid velocity in the straight channel is expected to grow linearly with syringe height, which can be seen with the fitted trendline in the previous graph.

4.8 Bonus: Bernoulli Relation

Torricelli's law:

$$U \sim \sqrt{2g\Delta z}.$$

Thus,

$$U_3 \propto \sqrt{z_1}.$$

Comparing:

- Hagen–Poiseuille $\rightarrow U_3 \propto z_1$
- Bernoulli $\rightarrow U_3 \propto \sqrt{z_1}$

Differences arise because Bernoulli neglects viscous losses; Hagen–Poiseuille accounts for dissipation.

5 Channels of Different Size

5.1 Expected Velocity Ratio

Flow rate continuity requires

$$U \propto \frac{1}{A}.$$

For a fixed height channel, area ratio approximates width ratio:

$$\frac{U_2}{U_1} \approx \frac{W_1}{W_2}.$$

This assumes Newtonian behavior. Thus, with a starting width of 241.197 micrometers and a expansion width of 507.619 micrometers, the theoretical centerline flow velocity ratio is approximately 2.105.

5.2 Measured Ratio (Data Required)

Before the expansion, the measured velocity was 1005.823 micrometers/second, after the expansion, it is measured at 408.012 micrometers/second. This yields a velocity ratio of 2.465, which generally agrees with the theoretically calculated value.

5.3 Flow Features

Abrupt contractions create separated regions and recirculation; gradual transitions suppress separation and produce more ordered streaklines. In the abrupt transition, there are pockets of turbulent/circular flow at the edges of the expansion chamber. The differences can be clearly seen in the two following figures.

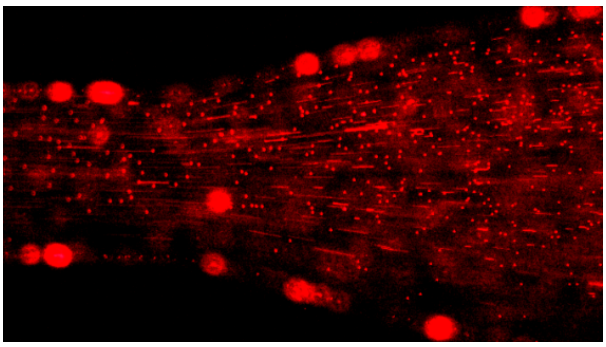

Figure 4: Smooth expansion

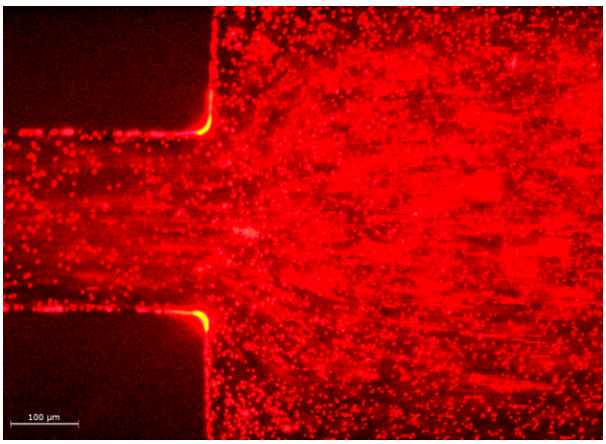

Figure 5: Abrupt expansion

5.4 Turbulence

Given Re $\ll$ 2000, turbulent flow is unlikely; streaklines should remain smooth. Localized disturbances do not constitute sustained turbulence.

5.5 Flow Transitions in Engineering

Smooth transitions reduce pressure loss and unsteadiness. Synthetic jets provide control authority to shape flow separation.

6 Channels with Bends

6.1 Velocity Change

Theory expects nearly unchanged centerline speed if cross-section remains constant. Curvature may induce secondary Dean vortices, resulting in flow velocity discrepancy. For the sharp bend channel, velocity before the bend was measured at 714.988 micrometers/second with valocity after the bend of 528.127 micrometers/second. For the curved bend channel, centerline velocities were measured at 560.019 micrometers/second and 694.1 micrometers/second before and after the bend, respectively.

6.2 Flow Features

Smooth bend → smooth pathlines; Sharp bend → recirculation, separation, secondary vortices. These can be seen in the following figures.

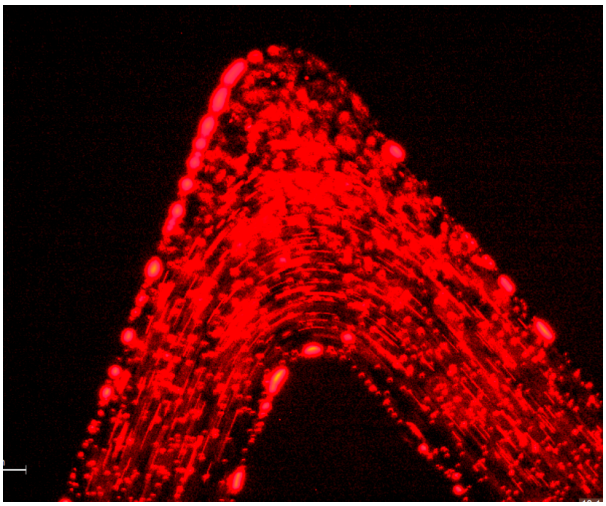

Figure 6: Smooth bend

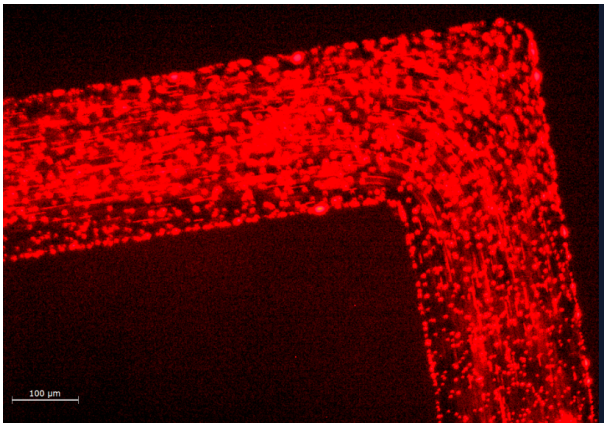

Figure 7: Sharp bend

6.3 Turbulence

Likely still laminar due to low Re. Observed waviness arises from curvature, not turbulence.

6.4 Concave vs. Convex Corners

Concave corners accelerate flow, yielding narrower stream tubes; convex corners slow flow and widen stream tubes.